Disruption of peroxisome proliferator–activated receptor γ coactivator (PGC)-1α reverts key features of the neoplastic phenotype of glioma cells

Received for publication, December 7, 2018 Published, Papers in Press, December 21, 2018, DOI 10.1074/jbc.RA118.006993

Ines Bruns[a,b,c,d1], **Benedikt Sauer**[a,b,c,d1], **Michael C. Burger**[a,b,c,d], **Jule Eriksson**[a,e], **Ute Hofmann**[f,g2], **Yannick Braun**[h], **Patrick N. Harter**[b,c,d,h3], **Anna-Luisa Luger**[a,b,c,d4], **Michael W. Ronellenfitsch**[a,b,c,d5,6], **Joachim P. Steinbach**[a,b,c,d6,7], **and Johannes Rieger**[a,i6]

From the [a]Dr. Senckenberg Institute of Neurooncology, University Hospital Frankfurt, Goethe University, 60528 Frankfurt, Germany, the [b]German Cancer Consortium (DKTK), Partner Site Frankfurt/Mainz, 60590 Frankfurt, the [c]German Cancer Research Center (DKFZ), 69120 Heidelberg, Germany, the [d]University Cancer Center (UCT), University Hospital Frankfurt, Goethe University, 60590 Frankfurt, Germany, the [e]Department of Neurology, University of Basel, 4031 Basel, Switzerland, the [f]Dr. Margarete Fischer-Bosch Institute of Clinical Pharmacology, 70376 Stuttgart, Germany, the [g]University of Tübingen, 72074 Tübingen, Germany, the [h]Institute of Neurology (Edinger Institute), University Hospital Frankfurt, Goethe University, 60528 Frankfurt, Germany, and the [i]Interdisciplinary Division of Neuro-Oncology, Hertie Institute of Clinical Brain Research, University Hospital Tübingen, 72076 Tübingen, Germany

Edited by Alex Toker

The peroxisome proliferator–activated receptor γ coactivator (PGC)-1α is a master regulator of mitochondrial biogenesis and controls metabolism by coordinating transcriptional events. Here, we interrogated whether PGC-1α is involved in tumor growth and the metabolic flexibility of glioblastoma cells. PGC-1α was expressed in a subset of established glioma cell lines and primary glioblastoma cell cultures. Furthermore, a higher PGC-1α expression was associated with an adverse outcome in the TCGA glioblastoma dataset. Suppression of PGC-1α expression by shRNA in the PGC-1α–positive U343MG glioblastoma line suppressed mitochondrial gene expression, reduced mitochondrial membrane potential, and diminished oxygen as well as glucose consumption, and lactate production. Compatible with the known PGC-1α functions in reactive oxygen species (ROS) metabolism, glioblastoma cells deficient in PGC-1α displayed ROS accumulation, had reduced RNA levels of proteins involved in ROS detoxification, and were more susceptible to death induction by H_2O_2 compared with control cells. PGC-1αsh cells also had impaired proliferation and migration rates *in vitro* and displayed less stem cell characteristics. Complementary effects were observed in PGC-1α–low LNT-229 cells engineered to overexpress PGC-1α. In an *in vivo* xenograft experiment, tumors formed by U343MG PGC-1αsh glioblastoma cells grew much slower than control tumors and were less invasive. Interestingly, the PGC-1α knockdown conferred protection against hypoxia-induced cell death, probably as a result of less active anabolic pathways, and this effect was associated with reduced epidermal growth factor expression and mammalian target of rapamycin signaling. In summary, PGC-1α modifies the neoplastic phenotype of glioblastoma cells toward more aggressive behavior and therefore makes PGC-1α a potential target for anti-glioblastoma therapies.

This work was supported in part by Grant RI2175/1-1 from the Deutsche Forschungsgemeinschaft (DFG) (to J. P. S. and J. R.). J. P. S. and J. R. have served as consultants for Roche Applied Science, the European distributor of bevacizumab.

This article contains Figs. S1–S3 and Tables S1–S3.

[1] Both authors contributed equally as first authors.

[2] Supported by the Robert-Bosch Foundation, Stuttgart, Germany.

[3] Recipient of a fellowship from the University Cancer Center (UCT) Frankfurt.

[4] Recipient of funding from Frankfurt Research Funding within the framework of the "Sponsorship Model" and a fellowship in the program "Clinician Scientist" by the Else Kröner-Forschungskolleg (EKF), which is supported by The Else Kröner-Fresenius Foundation.

[5] Recipient of funding from the Medical Faculty, University Hospital Frankfurt Program "Nachwuchsforscher 2012" as well as "Clinician Scientists Program", and a fellowship from the University Cancer Center (UCT) Frankfurt. To whom correspondence may be addressed: Dr. Senckenberg Institute of Neurooncology, University Hospital Frankfurt, Goethe University, Schleusenweg 2-16, 60528 Frankfurt, Germany. Tel.: 49-69-6301-87712; Fax: 49-69-6301-87713; E-mail: m.ronellenfitsch@gmx.net.

[6] These authors contributed equally as senior authors.

[7] Hertie Professor of Neurooncology. To whom correspondence may be addressed: Dr. Senckenberg Institute of Neurooncology, University Hospital Frankfurt, Goethe University, Schleusenweg 2-16, 60528 Frankfurt, Germany. Tel.: 49-69-6301-87712; Fax: 49-69-6301-87713; E-mail: joachim.steinbach@med.uni-frankfurt.de.

Changes in tumor metabolism are key events in the process of transformation (1, 2), and the adaptation to variable nutritional environments requires flexible and coordinated cellular responses toward a multitude of stress conditions. We have previously found that glioblastoma cells under starvation conditions employ mitochondrial respiration to achieve energy homeostasis. This response is supported by WT *p53* and its effectors SCO2 and TIGAR (3, 4). Furthermore, there is an inverse relationship between the activity of the growth-promoting EGFR[8]/Akt/mTOR pathway and survival under nutri-

[8] The abbreviations used are: EGFR, epidermal growth factor receptor; mTOR, mammalian target of rapamycin; ACC, acetyl-CoA carboxylase; Akt, protein kinase B; pAkt, phosphorylated Akt; MT-CO, mitochondrially encoded cytochrome *c* oxidase subunit; ERRα, estrogen-related receptor; ROS, reactive oxygen species; SFM, serum-free medium; sh, short hairpin; 2-NBDG, 2-(*N*-(7-nitrobenz-2-oxa-1,3-diazol-4-yl)amino)-2-deoxyglucose; DMEM, Dulbecco's modified Eagle's medium; H_2DCFDA-AM, 2′,7′-dichlorodihydrofluorescein diacetate-acetoxymethyl ester; DCF, 2′,7′-dichlorodihydrofluorescein; TMRM, tetramethylrhodamine; FCS, fetal calf serum; VEGF, vas-

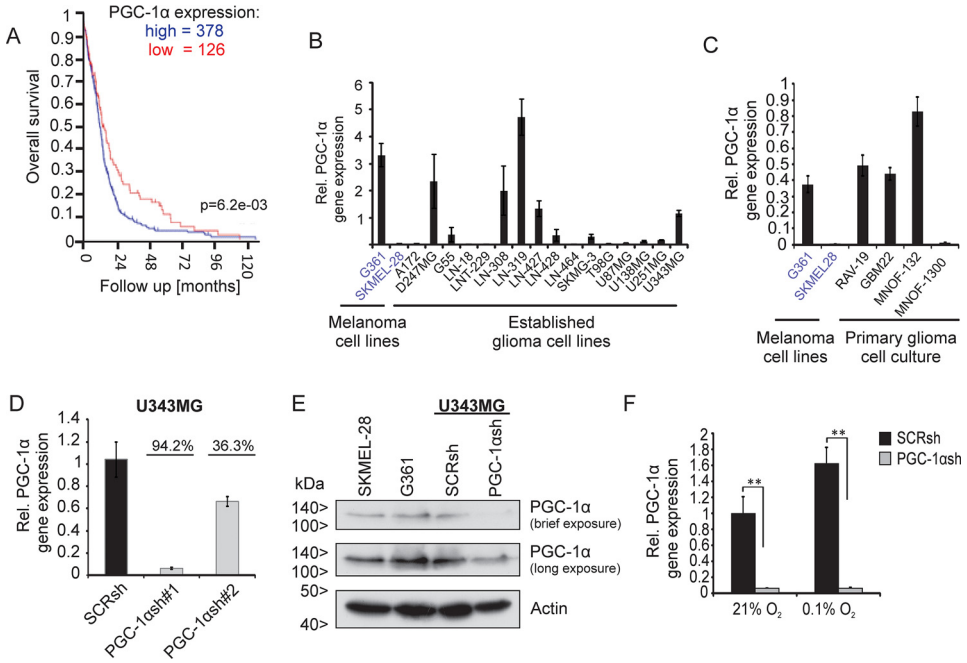

Figure 1. Knockdown of PGC-1α in the U343MG glioblastoma cell line. *A,* R2 database analysis shows negative correlation between PGC-1α expression and survival in glioma patients. The investigation was performed using only glioblastoma samples and the dataset "Tumor Glioblastoma–TCGA–540–MAS5.0–u133a" in the R2 database using overall survival data and 1st quartile of gene expression as a cutoff parameter. *B* and *C*, established glioma cell lines (*B*) and primary glioblastoma cell cultures (*C*) were analyzed for PGC-1α mRNA expression by qPCR. The melanoma cell line G361 served as positive and SKMEL-28 as negative control for PGC-1α expression. *D,* quantitative qPCR analysis confirms knockdown of PGC-1α in U343MG glioma cell line. *E,* SKMEL-28, G361, and U343MG SCRsh and PGC-1αsh#1 cells were incubated for 24 h in SFM, and PGC-1α and actin were analyzed by immunoblot. *F,* PGC-1α expression in SCRsh and PGC-1αsh#1 cells under normoxic conditions (21%) was compared with hypoxic conditions (0.1%), cells were incubated in serum-free medium.

ent depletion (5–7). One of the most important mediators of metabolic adaptation is the transcriptional coactivator peroxisome proliferator-activated receptor γ coactivator (PGC)-1α. It belongs to the PGC family and, in a tissue-specific manner, is responsive to different physiological stimuli like nutrient supply and oxygen concentration. PGC-1α itself has no DNA-binding activity but coactivates a large repertoire of transcription factors, most of which belong to the nuclear respiratory family (NRF) (8, 9). Its interaction with NRFs leads to an increased expression of mitochondrial genes and proliferation. As such, PGC-1α is a mediator of mitochondrial biogenesis and oxidative phosphorylation and is therefore frequently regarded as a master regulator of mitochondrial function in mammals (9, 10). PGC-1α is abundantly expressed in highly oxidative tissues like the embryonic brown adipose tissue, heart and skeletal muscle cells, kidney, and to a lesser extent in brain (9, 11–13). According to the tissue where it is expressed, PGC-1α activity is induced by increased energy demand, such as cold temperature and exercise, or when energy yield needs to be optimized, during fasting (7, 12, 14). Another function of PGC-1α is the regulation of antioxidative responses and coordination of post-transcriptional events (15, 16). To fulfill its function as a flexible metabolic regulator, the activity of PGC-1α is regulated by diverse proteins like the AMP-activated protein kinase (AMPK), p38 MAPK, Akt, and GSK3β (17–20). Phosphorylation of PGC-1α by these proteins can activate or inhibit PGC-1α's activity and thereby influence cellular growth and metabolism. Since we previously found that Akt/mTOR and AMPK have profound effects on the growth, metabolism, and resistance of glioblastoma cells against hypoxia (5, 6, 21) and these kinases converge on PGC-1α, we here investigated the role of PGC-1α for metabolism and the neoplastic phenotype of glioblastomas.

Results

PGC-1α is expressed in glioblastomas and associated with reduced survival

To investigate expression and relevance of PGC-1α in glioblastomas, R2 database analysis was performed. This showed that survival of glioblastoma patients with high PGC-1α expression level was shorter than that of patients with low PGC-1α expression (Fig. 1*A*). Compared with glioblastomas, WHO°II and III gliomas have an increased expression of PGC-1α (Fig. S1*A*). PGC-1α was also reduced in glioblastomas compared with nontumor tissue (Fig. S1*B*).

We next tested whether PGC-1α was expressed in glioblastoma cell lines. Many glioblastoma cell lines and primary glioblastoma cell cultures showed elevated PGC-1α expression levels (Fig. 1, *B* and *C*). To gain insight into the function of PGC-1α in glioblastoma cells, the expression of PGC-1α was blocked by stable transfection with a short hairpin RNA (PGC-1αsh) plasmid in U343MG cells, which endogenously strongly expresses PGC-1α. At the mRNA level, PGC-1α expression was reduced by more than 94% in U343MG PGC-1α knockdown cells (PGC-1αsh) compared with control cells transfected with a plasmid

cular endothelial growth factor; PI, propidium iodide; PPP, pentose-phosphate-pathway; AMPK, AMP-activated protein kinase; NRF, nuclear respiratory family; SCRsh, scrambled shRNA sequence; bFGF-2, basic fibroblast growth factor-2; FFPE, formalin-fixed, paraffin-embedded; qPCR, quantitative PCR; PPAR, peroxisome proliferator-activated receptor.

coding a nontargeting scrambled shRNA sequence (SCRsh) (Fig. 1*D*). Immunoblot analysis confirmed the loss of PGC-1α in PGC-1αsh cells (Fig. 1*E*). Because it is known that hypoxia induces PGC-1α expression (26), PGC-1α gene expression was analyzed under hypoxia compared with normoxia. As expected, hypoxia substantially promoted PGC-1α expression in SCRsh cells but not in PGC-1αsh (Fig. 1*F*). Likewise, it has been reported previously that PGC-1β is abundantly expressed in highly oxidative tissues, which suggests that PGC-1β may also play an important role in mitochondrial biogenesis and function (22). In many of the glioma cell lines tested, PGC-1β was expressed at different levels (Fig. S1*C*). Thus, it was tested whether PGC-1α knockdown was compensated for by up-regulation of PGC-1β. However, the mRNA expression level of PGC-1β was similar in PGC-1αsh cells compared with SCRsh cells (Fig. S1*D*).

Knockdown of PGC-1α inhibits mitochondrial gene expression, diminishes oxygen as well as glucose consumption, and is accompanied by loss of ROS detoxification enzymes

Because of its essential role in mitochondrial biogenesis, the effect of PGC-1α knockdown on mitochondrial gene expression was analyzed. Depletion of PGC-1α profoundly down-regulated expression of most investigated genes coding for mitochondrial proteins (Fig. 2*A*). Interestingly, ATP synthase was not affected by the knockdown (Fig. 2*A*). The estrogen-related receptor-α (ERRα) and the nuclear respiratory factor-1 and -2 (Nrf-1 and Nrf-2) are known to be coexpressed and activated by PGC-1α, and by themselves they regulate PGC-1α expression (9, 23). We found that the expression levels of these PGC-1α–interacting genes were decreased in U343MG PGC-1αsh cells (Fig. 2*A*, *right*). Furthermore, reduction of mitochondrial membrane potential confirmed that PGC-1α depletion leads to mitochondrial dysfunction (Fig. 2*B*). To clarify whether this resulted in reduced cellular respiration, the oxygen consumption of both cell lines was analyzed. Indeed, PGC-1αsh cells had a much lower oxygen consumption rate compared with control cells (Fig. 2*C*). Besides its function in mitochondrial biogenesis, PGC-1α has additional metabolic functions, including the regulation of glucose transporter expression (24). Because glucose transporter 1 and 3 (GLUT-1/-3) are the predominantly existing glucose transporters in the brain and overexpression of these transporters is accompanied by poor prognosis in several solid tumors (25–27), expression of these transporters was analyzed in normoxia and hypoxia. As shown in Fig. 2*D*, both glucose transporters were up-regulated in hypoxia, but PGC-1α–depleted cells induced *GLUT-1* and *GLUT-3* expression to a significantly lesser extent compared with control cells. Furthermore, measuring glucose uptake with the fluorescent glucose analog 2-NBDG showed that PGC-1αsh cells had much lower glucose uptake compared with SCRsh cells (Fig. 2*E*). Additionally, PGC-1αsh cells consumed less glucose and secreted less lactate than control transfectants (Fig. 2, *F* and *G*). Because PGC-1α might affect ROS levels by modulating oxidative phosphorylation and ROS-detoxifying enzyme expression, ROS levels in both cell lines were analyzed by H_2DCFDA staining (Fig. 2*H*). Interestingly, cells lacking PGC-1α expression had only slightly higher ROS levels under normoxia but much higher ROS levels under hypoxia. The gene expression of the ROS detoxification enzymes superoxide dismutase 1 and 2 (*SOD1* and *SOD2*), but not catalase, were significantly down-regulated in PGC-1αsh cells (Fig. 2*I*). To assess the functional relevance of the reduced *SOD1* and *SOD2* expression, cells were exposed to exogenous H_2O_2. Indeed, PGC-1αsh cells were more susceptible to cell death induction by H_2O_2 addition than control cells (Fig. 2*J*).

PGC-1α–deficient cells are able to maintain energy homeostasis under hypoxic conditions

As PGC-1αsh cells were less glycolytic and also displayed reduced respiratory function, we were interested in the energy level of these cells and asked whether these cells activate alternative pathways. The previous results demonstrated that PGC-1αsh cells are less metabolically active, suggesting that they should be less vulnerable to starvation conditions. Hence, the level of ATP, AMP, and different intracellular metabolites was analyzed. As hypothesized, the lower metabolic activity of the PGC-1α–suppressed cells led to a preserved ATP level and energy charge under hypoxia (Fig. 3*A*), and many metabolites were down-regulated in the PGC-1αsh cells under normoxia (Fig. 3, *A–C*). Interestingly, the metabolites fumarate, malate, citrate, and α-ketoglutarate of the citric acid cycle (Fig. 3*B*) and the metabolites ribulose 5-phosphate and 6-phosphogluconate of the pentose-phosphate pathway (PPP) (Fig. 3*C*) displayed hypoxia-driven up-regulation exclusively in PGC-1αsh cells.

Knockdown of PGC-1α leads to attenuation of the neoplastic phenotype and loss of stem-like features

Invasive cancer cell lines use PGC-1α and its enhanced activity for mitochondrial biogenesis to promote growth and metastasis (10). Thus, we hypothesized that PGC-1α could play an important role in the proliferation and motility of glioblastoma cells. Using crystal violet staining, cell growth was analyzed. At all time points analyzed, PGC-1αsh cells grew much slower compared with control cells (Fig. 4*A*). Similar results were obtained with the BrdU colorimetric proliferation assay (Fig. 4*B*). In clonogenic assays, the formation of cell colonies of PGC-1αsh cells was inferior compared with control cells (Fig. 4*C*). Moreover, migration assays revealed a trend for fewer migrated PGC-1αsh cells under normoxic conditions compared with control cells, but this effect was not significant (Fig. 4*D*, *left*). As expected, hypoxia increased migration in control cells, and this was significantly diminished in PGC-1αsh cells (Fig. 4*D*, *right*). Because PGC-1α has been shown to positively regulate *VEGF* gene expression in cultured muscle and skeletal muscle cells (28), the mRNA level of *VEGF* was tested in U343MG cells (Fig. 4*E*). As hypothesized, *VEGF* gene expression was substantially reduced in PGC-1αsh cells. Because primary glioblastoma cell cultures had higher PGC-1α expression levels compared with established cell lines (Fig. 1*C* and Fig. S2), it was examined whether PGC-1α was involved in the propagation of the stem cell phenotype. We therefore investigated whether suppression of PGC-1α expression had an impact on tumor spheroid formation under stem cell culture conditions. Interestingly, PGC-1αsh cells were no longer able to form tumor spheres under

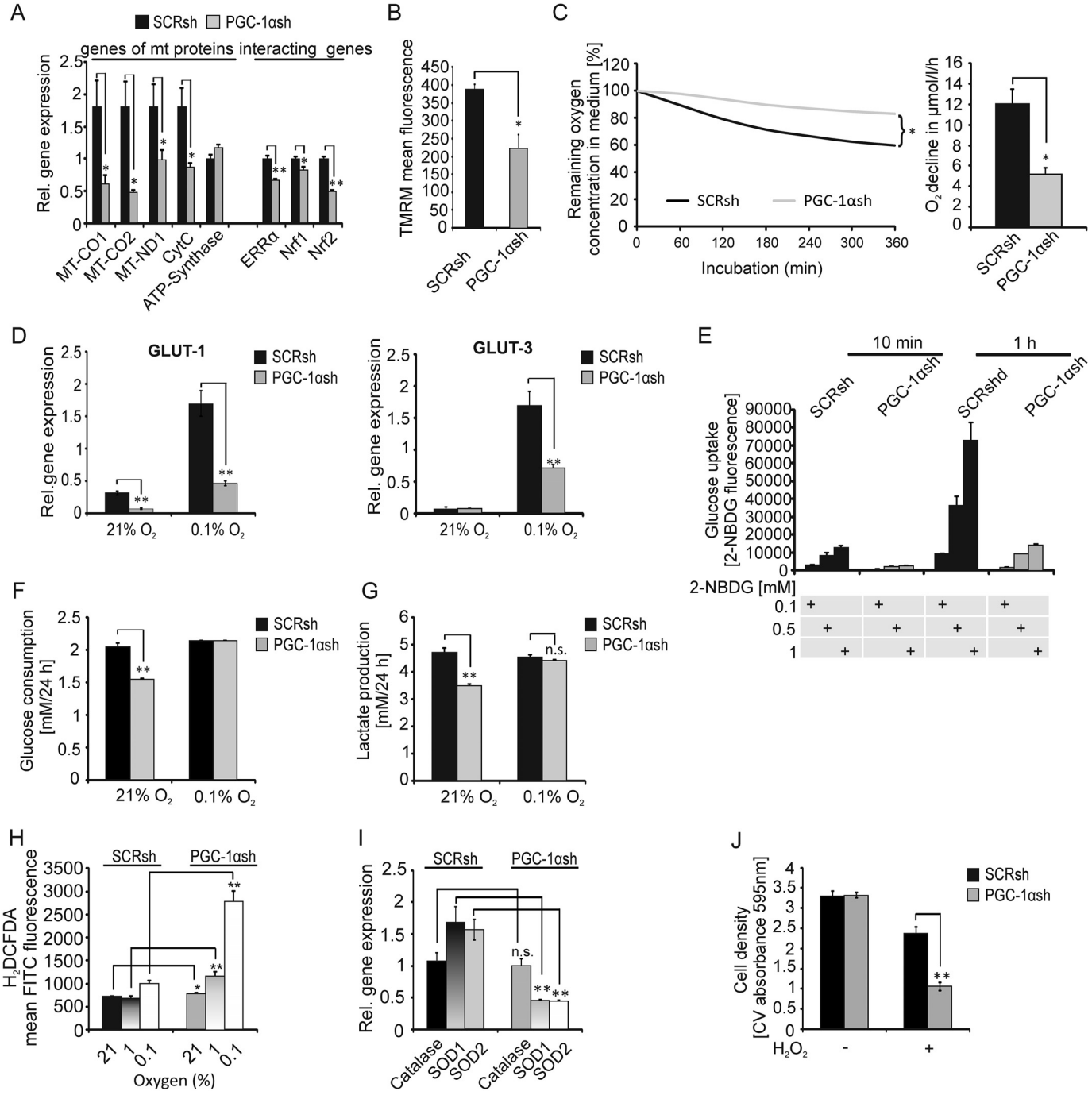

Figure 2. PGC-1α expression is necessary for mitochondrial respiration, glucose uptake, and ROS defense. *A,* expression of genes of mitochondrial (*mt*) proteins (*MT-CO1, MT-CO2, MT-ND1, CytC,* and *ATP* synthase) as well as of genes that interact with PGC-1α (*ERRα, Nrf1,* and *Nrf2*) was quantified by qPCR in nontargeting scrambled (SCRsh) cells compared with PGC-1α-suppressed (PGC-1αsh) cells. *B,* for mitochondrial membrane analysis, cells were incubated for 30 h in SFM, stained with TMRM, and measured by flow cytometry analysis. *C,* U343MG SCRsh and PGC-1αsh cells were incubated for 6 h, and oxygen consumption was measured by the fluorescent base PreSens System, and a representative section is shown. *D, GLUT-1* and *GLUT-3* expression under SFM with 2 mM glucose and in the presence of normoxia or hypoxia was analyzed by qPCR analysis. *E,* cells were incubated with 2-NBDG as indicated in SFM with 2 mM glucose for 10 min and 1 h, and glucose uptake was measured by flow cytometry analysis using the fluorescent glucose analog. *F* and *G,* cells were exposed to restricted glucose (2 mM) in SFM for 24 h at normoxic or hypoxic conditions, and the remaining glucose (*F*) or lactate (*G*) was measured in the medium. *H,* after 30 h of incubation at 21, 1, or 0.1% oxygen in SFM, cells were stained with the fluorescent H_2DCFDA ROS indicator and analyzed by flow cytometry analysis. *I,* expression of catalase, *SOD1*, and *SOD2* mRNA was analyzed by qPCR. *J,* U343MG SCRsh and PGC-1αsh cells were exposed to 0.8 mM H_2O_2 for 4 h, and cell density was examined by crystal violet (*CV*).

these conditions (Fig. 4*F*). Similarly, quantitative real-time mRNA expression revealed that up-regulation of the brain stem cell factors podoplanin, musashi-1, and *Sox2* was suppressed in the PGC-1αsh cells (Fig. 4*G*). Immunoblot analysis further verified this effect (Fig. 4*H*). Suppression of PGC-1α also inhibited the phosphorylation of Akt in U343MG cells cultured in stem cell medium, whereas the phosphorylation of ACC was unaffected (Fig. 4*H*). These cumulated results led us to conclude

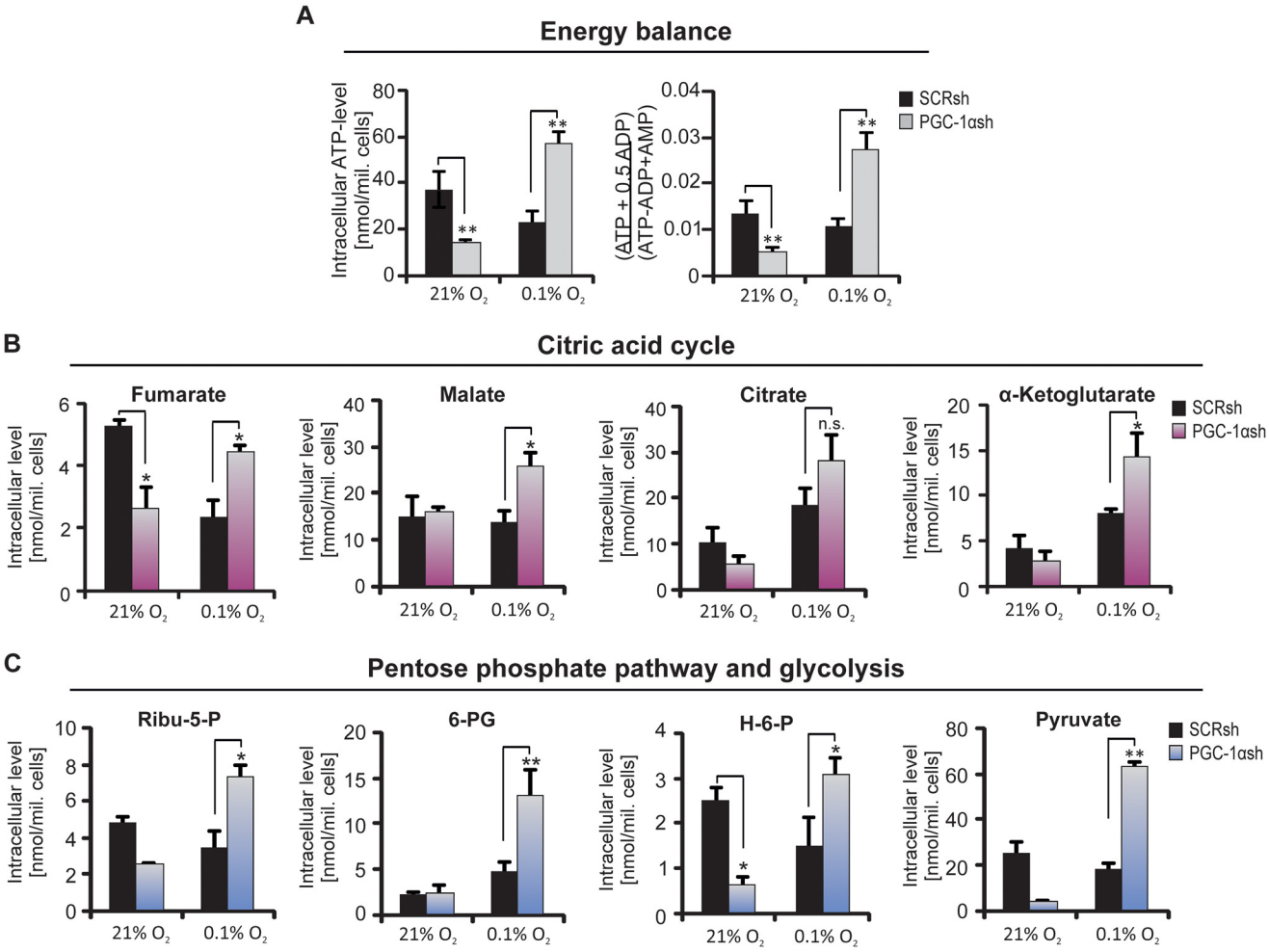

Figure 3. Alterations in the level of intracellular metabolites. The quantification of different intracellular metabolite levels in PGC-1αsh cells compared with the corresponding control cells under serum-free conditions and in the presence or absence of oxygen are shown. *A,* ATP level (*left*) and the energy charge (*right*). *B,* metabolites of the citric acid cycle (fumarate, malate, citrate, and α-ketoglutarate). *C,* metabolites of the pentose phosphate pathway (*PPP*) and glycolysis, ribulose 5-phosphate (*Ribu-5-P*), and 6-phosphogluconate (*6-P-G*) as well as hexose 6-phosphate (*H-6-P*) and pyruvate.

that the loss of PGC-1α leads to a less aggressive tumor phenotype. We further investigated this hypothesis in an *in vivo* orthotopic xenograft experiment. When SCRsh and PGC-1αsh cells were implanted intracranially in nude mice, survival was much longer in animals carrying PGC-1αsh tumors ($p < 0.002$, log rank) (Fig. 4*I*); these animals had a median survival of 79 days compared with 42 days in the control group bearing SCRsh cell tumors. Interestingly, U343MG SCRsh cells displayed invasive tumor margins with satellites of tumor cells migrating into the host brain, whereas the PGC-1αsh cells had smooth tumor margins. Immunohistochemistry staining for the proliferation marker Ki67 revealed no obvious difference between the tumors formed by SCRsh and PGC-1αsh cells at the time of sacrifice (Fig. 4*J*).

Loss of PGC-1α is accompanied by impaired EGFR expression and signal transduction

Aggressive tumor growth typically is associated with formation of necroses *in vivo*, reflecting the defunct sensing or coupling of growth-inhibitory signals from the microenvironment. Based on the energy-consuming features of PGC-1α– high cells and the improved energy homeostasis in PGC-1αsh cells, we hypothesized that this would result in differential susceptibility toward hypoxia-induced cell death. Indeed, depletion of PGC-1α profoundly protected the cells against hypoxia-induced cell death (Fig. 5*A*). Immunoblot analysis indicated that cells lacking PGC-1α had much less hypoxia-inducible factor-1α (HIF-1α) induction, pointing to a disruption of hypoxia-induced signal transduction (Fig. 5*B*). Furthermore, phosphorylation of the protein kinase B (Akt) and the AMPK downstream target ACC was strongly reduced in PGC-1α knockdown cells. Akt phosphorylation is, among others, affected by mTOR complex 2. Activated Akt inactivates the TSC1/TSC2 complex through phosphorylation of TSC2 and thereby promotes the activation of the mTOR complex 1 (29). We have shown earlier that the inhibition of EGFR, Akt, or mTOR confers resistance against hypoxia-induced cell death (6, 21). Thus, we investigated whether the pAkt downregulation contributes to the resistance against hypoxia-induced cell death mediated by PGC-1α knockdown. For this, U343MG SCRsh cells were treated with the Akt inhibitor AktVIII, which induced a significant reduction in hypoxia-induced cell death compared with vehicle-treated cells (Fig.

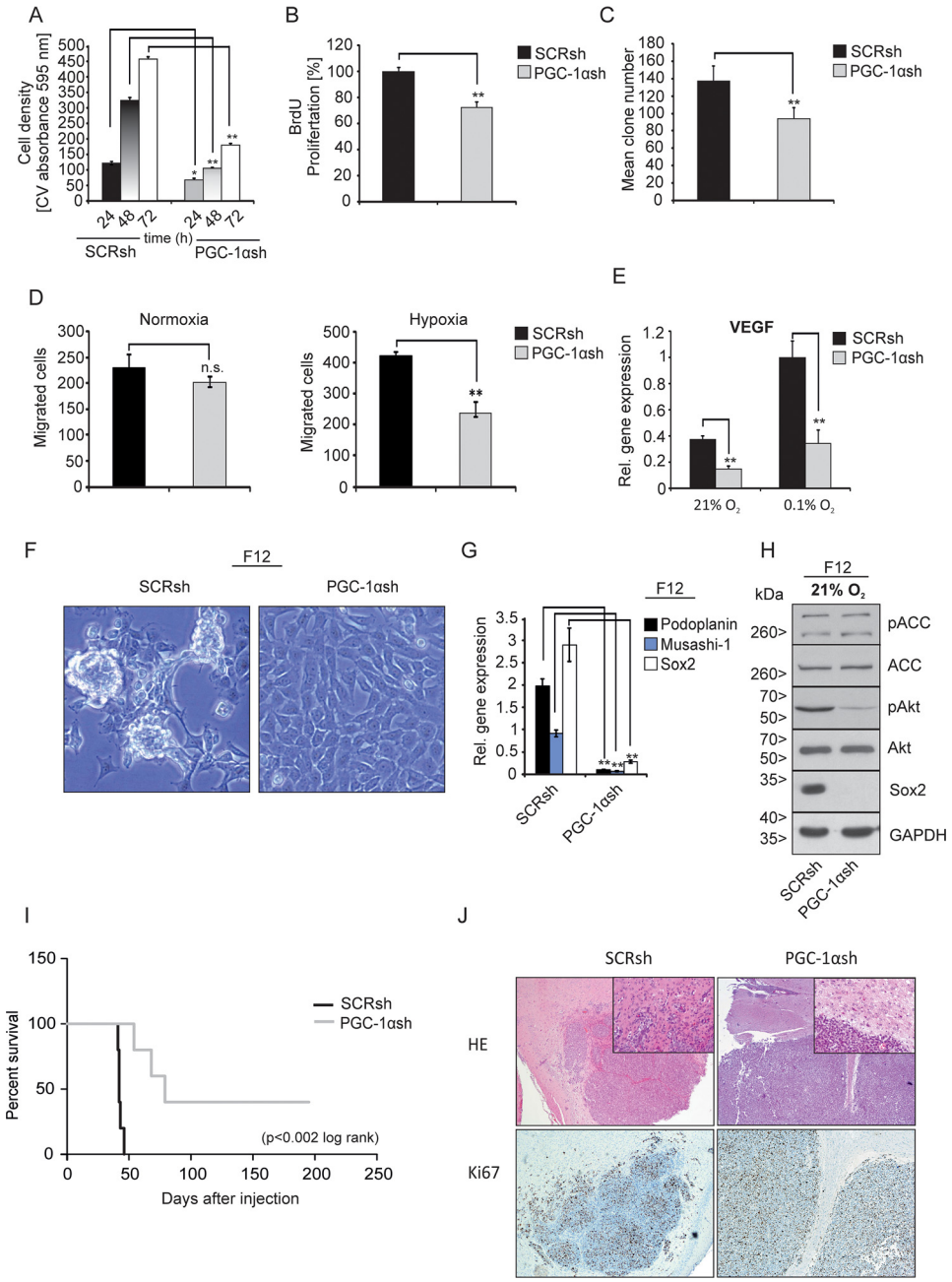

Figure 4. PGC-1α suppression diminishes cell migration and tumor formation and leads to loss of spheroid formation. *A,* for cell growth analysis, cells were normalized to cell density at time point 0 before starting the experiment; cells were cultivated with standard DMEM (including FCS and supplemented with high glucose) and were stained with crystal violet after 24, 48, and 72 h. *B,* cell proliferation was measured by BrdU colorimetric assay after 24 h of incubation with BrdU. *C,* evaluation of the clone formation ability under normoxic conditions with standard cell culture medium containing 10% FCS. *D,* cells were incubated under normoxia (*left*) or hypoxia (*right*), and the number of migrated cells was counted. *E,* VEGF gene expression was analyzed by qPCR under normoxia or hypoxia and 2 mM glucose in SFM. *F,* U343MG SCRsh (*left*) and PGC-1αsh (*right*) cells were cultivated in DMEM/F-12 medium (stem cell medium), and representative phase-contrast microscopic images are shown. *G,* expression of the stem cell factors Podoplanin, Musashi-1, and Sox2 in SCRsh and PGC-1αsh cells was analyzed by qPCR analysis. *H,* cells were treated for 24 h with DMEM/F-12 medium; the protein level of Sox2, pACC, ACC, pAkt, and Akt was analyzed by immunoblot analysis. *I,* Kaplan-Meier curve of nude mice which were intracranially injected with either SCRsh or PGC-1αsh cells. *J,* tissue staining with H&E (above) and immunohistochemical staining for Ki67 (below) of sections of U343MG SCRsh and PGC-1αsh tumors. *Insets* show magnifications of the tumor borders.

5*C*). Taken together, PGC-1αsh cells displayed a number of phenotypes that could be linked to reduced EGFR signaling. Therefore, we examined *EGFR* expression in PGC-1αsh cells and confirmed a massive down-regulation of *EGFR* expression at the mRNA level (Fig. 5*D*) as well as at the protein level (Fig. 5*E*). Next, it was examined whether PGC-1α knockdown-mediated suppression of *EGFR* influences the resistance of glioblastoma cells against EGFR inhibition. As indicated by PI-FACS analysis, addition of PD153035 or erlotinib did not further reduce hypoxia-induced cell death in PGC-1αsh cells indicating redundant pathways (Fig. 5*F*). In control cells, EGFR inhibition mediated the previously described protection against hypoxia-induced cell death (21). Downstream EGFR signaling was likewise down-regu-

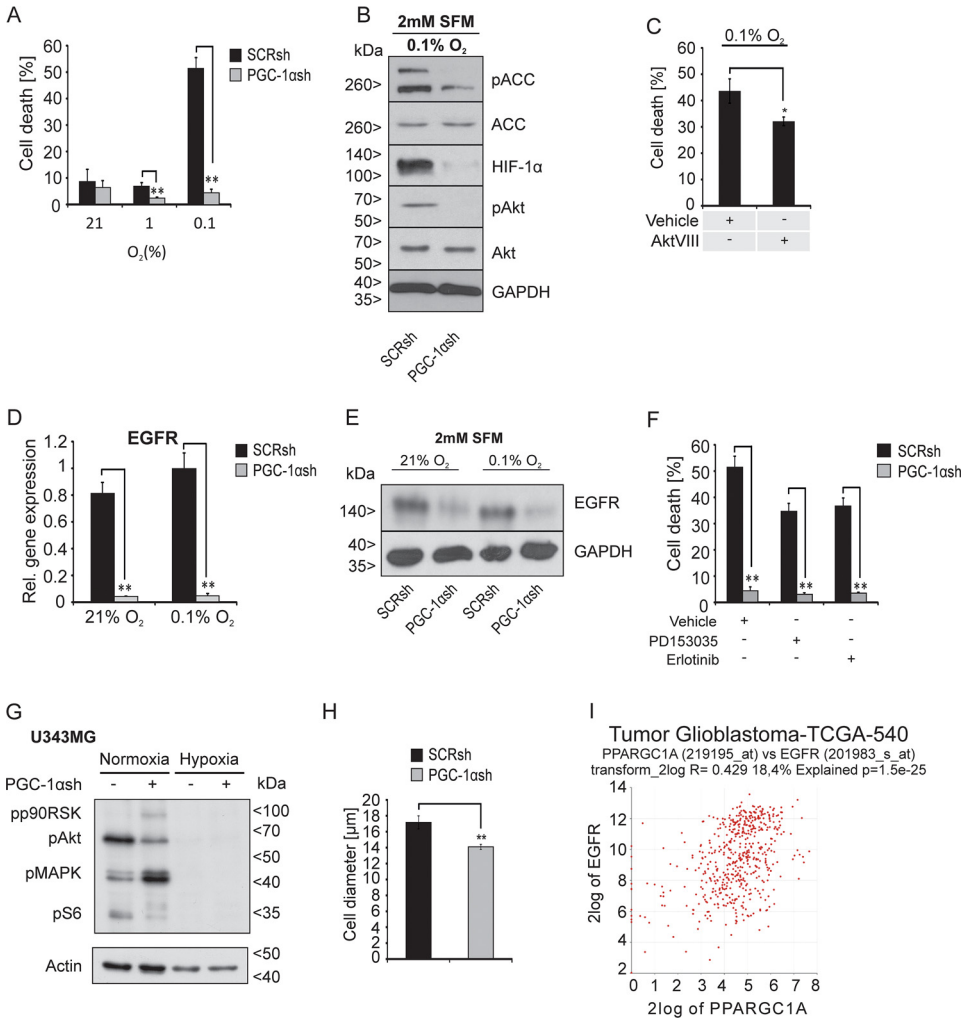

Figure 5. Cells lacking PGC-1α are strongly protected against hypoxia-induced cell death and exhibit down-regulation of the EGFR. *A,* cells were incubated at 21, 1, or 0. 1% oxygen in SFM for 30 h, stained with PI, and analyzed by flow cytometry analysis, where PI-positive cells were rated as dead cells. *B,* cells were exposed to SFM under 0.1% oxygen for 24 h, and the protein expression of HIF-1α, pACC, ACC, pAkt, and Akt was determined by immunoblot analysis. *C,* cells were treated with vehicle (DMSO) or AktVIII (10 μM) for 30 h under SFM and hypoxia, and cell death was analyzed by PI-FACS. *D,* expression of *EGFR* in SCRsh and PGC-1αsh cells after exposure to SFM (2 mM) and 21 or 0.1% oxygen for 24 h was analyzed by qPCR (*D*) and immunoblot analysis (*E*). *F,* SCRsh cells were treated with vehicle (DMSO) or with the EGFR inhibitors PD153035 (10 μM) and Erlotinib (10 μM) for 30 h at 2 mM glucose in SFM, and cell death was analyzed by PI-FACS. *G,* LNT-229 SCRsh and PGC-1αsh cells were incubated for 8 h in SFM with 2 mM glucose in normoxia or hypoxia, and downstream signaling of the EGFR was examined by immunoblot analysis of phosphorylated $p90^{RSK}$, phosphorylated Akt (*pAkt*), phosphorylated ERK1/2 (*pMAPK*), and phosphorylated S6 protein (*pS6*), and actin served as internal control. *H,* cell pellets of SCRsh and PGC-1αsh cells were used for evaluation of the cell size by light microscopy and analysis software (Olympus). *I, in silico* analysis using the R2 database displays a correlation between PGC-1α and *EGFR* expression in glioma patients. The investigation was performed also using only glioblastoma samples and the dataset "Tumor Glioblastoma–TCGA–540–MAS5.0–u133a" in the R2 database.

lated in the PGC-1αsh cells, including decreased phosphorylation of the canonical mTORC1 target and effector RPS6 (ribosomal protein S6) (Fig. 5*G*). Interestingly, congruent to the attenuation of mTOR signaling, PGC-1αsh cells had decreased cell size both *in vitro* (Fig. 5*H*) and *in vivo* (data not shown). Further *in silico* analysis using the R2 database indicated a significant correlation between *EGFR* and PGC-1α expression in glioblastomas (Fig. 5*I*).

PGC-1α overexpression in LNT-229 glioblastoma cells

To substantiate the previous results, it was investigated whether ectopic overexpression of PGC-1α leads to opposite effects compared with knockdown of PGC-1α. Therefore, the impact of ectopic PGC-1α expression was analyzed in LNT-229 cells that endogenously exhibit low PGC-1α expression (Fig. 1*B*). Cells were transfected with either a control (pcDNA3.1) or PGC-1α (pcDNA3.1) expression plasmid (Fig. S3*A*). LNT-229 cells with high PGC-1α expression had an increased respiration rate compared with control cells (Fig. S3*B*). Furthermore, these cells were more resistant to exogenous H_2O_2 treatment (Fig. S3*C*), and accordingly, PGC-1α–overexpressing cells showed higher levels of all three analyzed ROS-defense enzymes (Fig. S3*D*). Next, we investigated whether expression of PGC-1α modulates cell proliferation, and indeed, cells with high PGC-1α expression showed increased cell density compared with control cells (Fig. S3*E*). Interestingly, PGC-1α–overexpressing cells were markedly more sensitive to hypoxia-induced cell death (Fig. S3*F*), whereas strong hypoxia resistance was observed in PGC-1αsh cells (Fig. 5*A*). In summary, overexpression of PGC-1α in LNT-229 cells induced a complementary

phenotype compared with knockdown of PGC-1α in U343MG cells.

Discussion

In contrast to the historic view that cancer cells rely predominantly on glycolysis, research within the last decade has demonstrated that many cancer types utilize fatty acid oxidation and mitochondrial metabolism through the citric acid cycle for their anabolic needs and oxidative phosphorylation for efficient ATP production (30). This has also been shown for gliomas (31–34). To sustain oxidative phosphorylation, cells need to orchestrate a complex network of cellular pathways. Because PGC-1α has been found to play a major role in promoting oxidative phosphorylation in other solid tumors (35, 36), we here investigated the function of PGC-1α in GBM cells. Based on these considerations, we hypothesized that PGC-1α could be involved in controlling glioblastoma cell growth and energy homeostasis. PGC-1α was expressed in a subset of established glioblastoma cell lines, and its expression was enhanced by hypoxia (Fig. 1) (37).

In accordance with its well-established functions in the regulation of mitochondrial biogenesis in other cancer cell types, suppression of PGC-1α reduced gene transcription of diverse mitochondrial proteins leading to a decrease of the mitochondrial membrane potential as well as the cellular respiration rate (Fig. 2, *A–C*). In line with published results indicating that PGC-1α is involved in *Glut-4* expression (38), we found a down-regulation of *GLUT-1* and *GLUT-3* gene expression, the dominant glucose transporters in brain (39), in PGC-1αsh cells and less induction of *GLUT-1* by hypoxia (40). Consistent with the lower glucose transporter gene expression, PGC-1αsh cells showed reduced uptake of glucose from the medium. This is likely responsible for our observation that although PGC-1αsh cells exhibited deficient mitochondrial respiration, there was no compensatory increase in glycolysis (Fig. 2, *D* and *E*). Several studies demonstrated that PGC-1α gene expression is increased in response to oxidative stress and that ROS-detoxifying enzymes like SOD1, SOD2, and catalase are up-regulated by PGC-1α (41–43). In accordance with this, in PGC-1α–suppressed cells we found an accumulation of ROS, and these cells were more susceptible to H_2O_2. This could be explained by diminished gene expression of SOD1 and SOD2 (Fig. 2, *H–J*). Therefore, PGC-1α appears to be important for the regulation of ROS detoxification in GBM cells via *SOD1* and *SOD2*. ROS are also involved in intracellular signaling pathways and act as second messenger (44, 45). For that reason, it appears possible that ROS accumulation potentially promotes autophagy and other cytoprotective effects under starvation conditions (46–48).

We hypothesized that this diminished metabolism results in less energy consumption in PGC-1αsh cells. Indeed, the primary finding of metabolic profiling was that PGC-1αsh cells were able to preserve their ATP levels under hypoxic conditions, conferring a survival advantage against nutrient and oxygen deprivation. We also observed elevated levels of metabolites of the PPP. Because one important function of the PPP is generation of NADPH that is pivotal for ROS scavenging, PGC-1αsh cells may compensate for the defect in their ROS-defense mechanism by an up-regulation of the PPP to achieve more NADPH. We also saw an increase in the steady-state concentrations of the analyzed citric acid cycle metabolites, which may be a result of accumulation due to reduced mitochondrial capacity in PGC-1αsh cells (Figs. 2, *A–C*, and 3).

How do the profound changes in metabolism conferred by suppression of PGC-1αsh impact on key features of the neoplastic phenotype? Proliferation, migration, and invasion all require both energy supply and substrates for anabolism, which, to a substantial extent, rely on mitochondrial function. Congruent with this, PGC-1αsh cells displayed reduced proliferation and migration *in vitro,* and their reduced expression of the angiogenic gene *VEGF* may also impact *in vivo* tumor aggressiveness (Fig. 4, *A–E*). Furthermore, it appears logical that a tumor population dependent on oxidative phosphorylation, *e.g.* with PGC-1α activation, needs to promote angiogenesis. Interestingly, PGC-1α also seems to be involved in stem cell features because knockdown of PGC-1α mediated a loss of tumor sphere formation and *Sox2* expression (Fig. 4, *F–H*). This is in line with the finding that, in MCF-7 breast cancer cells, the ERRα–PGC-1α signaling inhibitor XCT790 was able to block mammosphere formation by inhibiting mitochondrial function as well as activation of several stem cell-related signaling pathways (49). These profound perturbations of essential oncogenic signaling cascades translated into a much better survival of animals orthotopically grafted with PGC-1αsh cells. Notably, a less invasive growth pattern was also detectable in histological specimens derived from PGC-1αsh xenograft tumors (Fig. 4, *I* and *J*). These findings match those of LeBleu *et al.* (10) in breast cancer models. In summary, the neoplastic phenotype is driven by PGC-1α in line with the established role of metabolism as one pillar of the hallmarks of cancer (50). Aggressive tumor growth depends on sufficient oxygen and substrate supply. Highly proliferative and anabolic tumor cells therefore may be selectively vulnerable to starvation conditions. To elucidate the impact of PGC-1α on resistance toward hypoxia and nutrient deprivation, we used an established model system to characterize cell vitality under starvation conditions designed to match the glioblastoma microenvironment (3, 6, 21).

PGC-1αsh cells display less stem cell features and are less aggressive, and the observed reduced metabolic activity probably leads to reduced nutrient usage resulting in resistance against hypoxia (Fig. 5*A*). The validity of this finding is underscored by the demonstration that, in PGC-1α–low LNT-229 cells, overexpression of PGC-1α enhances hypoxia-induced cell death (Fig. S3*F*). This effect could potentially promote selection of cell death-resistant clones and therefore may limit the therapeutic benefit of inhibiting PGC-1α signaling. It is likely that multiple factors are involved in the phenomenon of hypoxia resistance in PGC-1αsh cells. The level of phospho-ACC, a direct downstream target of the energy stress sensor AMPK, was lower in PGC-1αsh cells, indicating preserved energy homeostasis as already demonstrated by measuring ATP and energy charge. PGC-1α–suppressed cells also had lower levels of phospho-Akt and HIF-1-α, drivers of glucose uptake, glycolysis, and angiogenesis (51–53). This is congruent to the reduced levels of glucose uptake and *VEGF* mRNA in these cells. Considering the pattern of signaling alterations and phenotypes

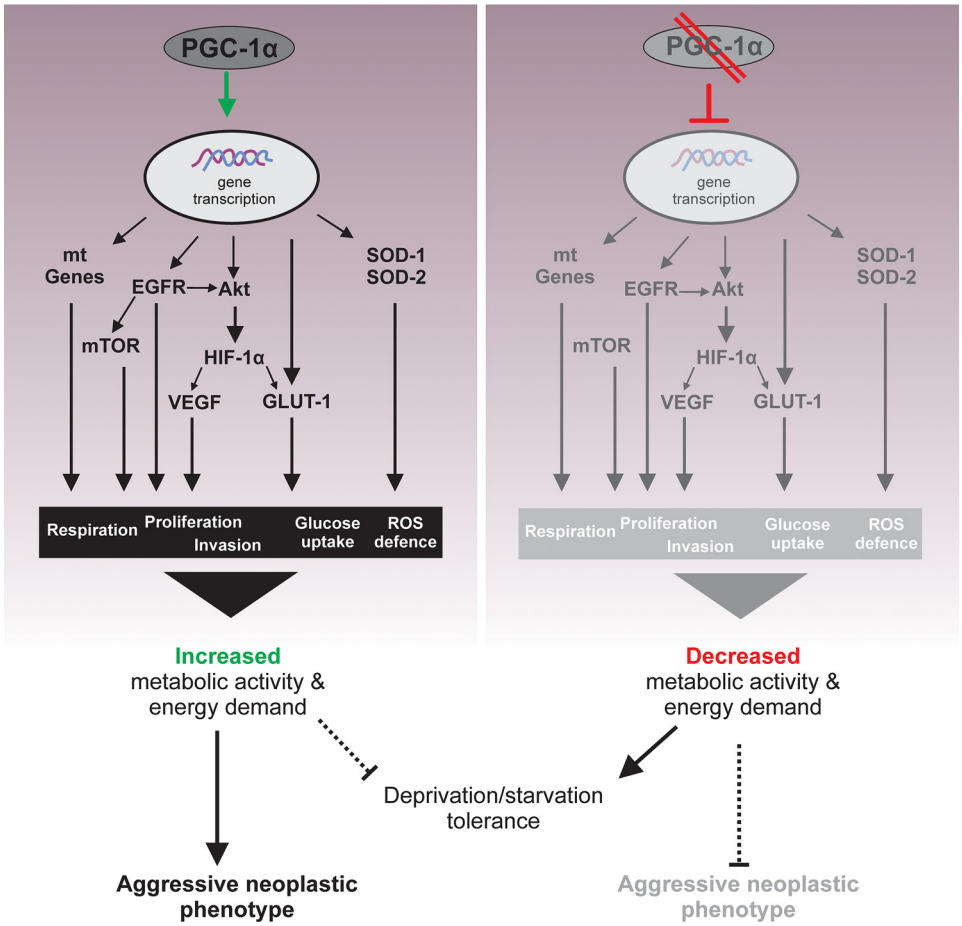

Figure 6. Schematic description of metabolic alterations caused by loss of PGC-1α expression. Suppression of PGC-1α leads to a broad range of metabolic changes. This includes the expression levels of pAkt and pACC, gene expression of mitochondrial proteins (mt Genes), ROS degradation enzymes (SOD-1 and SOD-2), and VEGF and of glucose transporters (GLUT-1 and GLUT-3). These alterations ascribe PGC-1α a major role in the response of glioma cells against starvation conditions and concurrently in the neoplastic cell growth.

observed in PGC-1αsh cells, there are many similarities with features found in cells exposed to EGFR inhibitors. We therefore investigated EGFR–mTOR signaling (6, 21) and indeed found a substantial down-regulation of total EGFR protein as well as of the mTOR effector phospho-RPS6 in PGC-1αsh cells (Fig. 5, *D–F*). The decrease in the cell size found in PGC-1αsh cells confirms the biological relevance of diminished mTOR signaling (Fig. 5*H*). An interaction between PGC-1α and EGFR has not been known previously, but the correlation between expression of PGC-1α and *EGFR* in our *in silico* analysis using the R-2 data platform support the validity of our findings *in vitro* (Fig. 5*I*). Regarding potential mechanisms of this interaction, further *in silico* analysis demonstrated that the PGC-1α promotor region contains binding sites for transcription factors that also occur in the promotor region of the *EGFR* and *GLUT-1* gene. Specifically, binding sites for PPAR-α, PPAR-γ1, and PPAR-γ2 can be found in the promotor region of PGC-1α. Furthermore, a PPAR-α–binding site is present in the *EGFR* promotor region. The *GLUT-1* gene may also be coregulated as binding sites for PPAR-γ1 and PPAR-γ2 occur in the promotor region of this gene (http://www.ensembl.org).[9] These transcription factors are also activated by PGC-1α which may result in a positive feedback loop. Interestingly, we have also recently found that, vice versa, activation of mTOR signaling by disruption of TSC2 induces PGC-1α expression and promotes an anabolic and oxidative phenotype (7). Intriguingly, in accordance with our key finding of PGC-1α as a driver of oxic and anabolic metabolism that promotes an aggressive phenotype, a proteomic analysis from the German Glioma Network has found that in tumor tissues from glioblastoma patients with short-term survival many proteins important for mitochondrial metabolism and oxidative phosphorylation were up-regulated in relation to samples from patients with long-term survival.[10] All key phenotypes observed in PGC-1αsh cells were analyzed in LNT-229 cells transfected with the PGC-1α expression plasmid (Fig. S3). The observation that PGC-1α expression led to opposite effects compared with knockdown of PGC-1α corroborated our findings obtained in the knockdown system.

The mechanisms and consequences of PGC-1α are summarized in Fig. 6. The coordinated regulation of parallel pathways by PGC-1α ultimately enables the oxidative and anabolic metabolism and results in an aggressive neoplastic phenotype. Alternatively, in the absence of PGC-1α, a catabolic, nonoxic

[9] Please note that the JBC is not responsible for the long-term archiving and maintenance of this site or any other third party hosted site.

[10] K. Stühler for the German Glioma Network, manuscript in preparation.

phenotype is promoted that confers resistance toward hypoxia and starvation conditions.

From a clinical perspective, PGC-1α is therefore an interesting target of antiglioblastoma therapies, although currently, there are no suitable strategies available to directly target PGC-1α. However, it should be cautioned that, as a trade-off, resistance toward hypoxia must be expected to occur as a consequence of PGC-1α inhibition. This has been shown previously for inhibition of EGFR, AKT, and mTOR, oncogenic kinases that drive anabolic metabolism and enhance consumption of energy and substrates (5, 6), and this should be considered in the choice of partners for combination therapy. Agents that may induce hypoxia, *i.e.* bevacizumab (54, 55), should be employed with caution in combination with anti-PGC-1α strategies.

Experimental procedures

Cell culture

The glioblastoma cell lines A172, LN-308, U138-MG, LN-18, LNT-229, and U251-MG were provided by Nicolas de Tribolet (Centre Hospitalier Universitaire Vaudois, Lausanne, Switzerland); the cell lines LN-319, LN-427, LN-428, LN-464, and T98G were provided by Monika Hegi (Laboratory for Tumor Biology and Genetics, Lausanne, Switzerland); the cell line D247MG was provided by Darell Bigner (Durham, NC); the cell line G55 was provided by Katrin Lamszus (Laboratory for Brain Tumor Biology, Hamburg, Germany); and the cell line U343MG was provided by Werner Paulus (Institute of Neuropathology, University Münster, Germany). SKMG-3 cells were provided by Joon Uhm (Mayo Clinic, Rochester, MN). U87MG cells were purchased from the ATCC. The melanoma cell lines SK-MEL-28 and G361 were used as positive and negative controls for PGC-1α expression and were provided by Stefan Kippenberger (Clinic of Dermatology, Laboratory for Clinical and Biochemical Dermatology, University Hospital Frankfurt, Germany). G361 cells were cultured in RPMI 1640 medium containing 10% fetal calf serum (FCS), 2 mM glutamine, 11 mM glucose, 100 IU/ml penicillin, and 100 mg/ml streptomycin. All other cell line were cultured in Dulbecco's modified Eagle's medium (DMEM, Gibco ThermoFisher Scientific, Dreieich, Germany) containing 25 mM glucose, 100 IU/ml penicillin, 100 mg/ml streptomycin, and 10% FCS. If not otherwise noted, cells were seeded at a density of $0.7–0.8 \times 10^5$ cells/well in 24-well plates. When 6-well plates were used, 2.5×10^5 cells were seeded per well, and for 10-cm dishes, 15×10^5 cells were seeded per well. For starvation analysis, cells were cultured in DMEM without FCS where 2 mM glucose was added. For reasons of simplification, the medium for starvation conditions is termed serum-free medium (SFM) in the course of this work.

Primary cell culture

The glioblastoma-derived primary glioblastoma cell cultures GBM22 and MNOF132 were kindly provided by Stefan Momma (Institute of Neurology (Edinger Institute), University Hospital Frankfurt, Goethe-University, Frankfurt, Germany) and the MNOF1300 cell culture by Dr. Julia Tichy (Dr. Senckenberg Institute for Neurooncology, University Hospital Frankfurt, Goethe University, Frankfurt, Germany). The RAV19 cell culture was kindly provided by Arabel Vollmann-Zwerenz (Neurooncology, University of Regensburg, Germany). Cells were cultured in DMEM/F-12 medium containing 20 ng/ml epidermal growth factor (EGF) and human basic fibroblast growth factor-2 (bFGF-2, both from ReliaTech, Wolfenbüttel, Germany) as well as 20% BIT admixture 100 supplement (Pelo Biotech, Planegg/Martinsried, Germany). For experiments, the cells were harvested with accutase. EGF and bFGF-2 were supplemented twice per week.

Reagents

Cells were treated with DMSO as control, Erlotinib (10 μM, Sequoia Research, Pangbourne, UK), PD153035 (10 μM, Tocris, Bristol, UK), or Akt inhibitor VIII (10 μM, Calbiochem, San Diego).

Stable transfection

Stable knockdown of PGC-1α in U343MG WT cells was done with pLKO.1 short hairpin RNA (shRNA) plasmids (PGC-1αsh#1, TRCN000001165, and PGC-1αsh#2, TRCN000001166) from Sigma. As control, cells were transfected with a pLKO.1 plasmid coding a nontargeting shRNA sequence (Addgene catalog no. 1864). The transfection reagent PeqFect (Peqlab, Erlangen) was used according to the manufacturer's protocol. Puromycin (2 μg/ml) was added to the culture medium for selection of successfully transfected cells. All further experiments were done with the PGC-1αsh#1 cells, where depletion of PGC-1α was most successful. PGC-1αsh generated with the shRNA sequence #1 cells are termed PGC-1αsh cells, and control cells generated with a nontargeting shRNA sequence are termed SCRsh cells in this paper. Overexpression of PGC-1α in LNT-229 cells was induced by stable transfection with the vector pcDNA3.1 PGC-1α (clone ID: OHu27412D), ordered from GenScript (Piscataway, NJ). For use as vector control, the insert was deleted generating empty pcDNA3.1. Transfection was performed with Attractene transfection reagent (Qiagen, Hilden), and cells were exposed to G418 (400 μg/ml) for selection.

Induction of hypoxia

Moderate hypoxia (1% O_2) was induced in a CO_2 incubator (Binder, Germany), and strong hypoxia (0.1% O_2) was induced by GasPak pouches for anaerobic culture (BD Biosciences, Heidelberg, Germany) (56).

Oxygen consumption

Oxygen measurements were done with the PreSens SDR SensorDish® reader (Regensburg, Germany). Cells were seeded in special 24-well sensor dishes. These dishes have a sensor spot at the bottom of each well. The wells were read out in 15-min intervals through the transparent bottom by a 24-channel SensorDish® Reader during the incubation. Before starting the experiment, medium containing FCS was freshly given to the cells, and each well was hermetically sealed with paraffin oil.

Cell death analysis

Cells were seeded in 24-well plates and allowed to attach. After 24 h, culture medium was removed, and cells were

washed with PBS. Thereafter, cells were treated with 2 mM glucose in serum-free medium and incubated at the denoted oxygen concentration for 30 h. Adherent cells as well as detached cells of the supernatant were pooled and stained with PI. The PI-positive cells were analyzed by FACS analysis as described previously (3).

Immunoblot analysis

For protein extraction, cells were seeded in 10-cm plates and treated as indicated. After 24 h, cells were washed with ice-cold phosphate-buffered saline (PBS) and lysed in RIPA lysis and extraction buffer (ThermoFisher Scientific). Protease and phosphatase inhibitor mixture (ThermoFisher Scientific) was freshly added. Lysate extraction and SDS-PAGE, antibody staining, and chemiluminescence protein detection were prepared as described previously (4). Primary and secondary antibodies that were used are listed in Tables S1 and S2).

RNA extraction and quantitative RT-PCR

One day before starting RNA extraction, cells were seeded in 6-well plates. RNA extraction, cDNA synthesis, and data analysis were performed as described previously (4). Used primer pairs are listed in Table S3.

Glucose/lactate measurements

For glucose and lactate measurements, cells were seeded in 24-well plates and allowed to attach for 24 h. Cells were treated with SFM containing 2 mM glucose. After an additional 24 h, the supernatant was collected, and cells were removed by centrifugation. Glucose and lactate concentrations were measured using the biochemistry analyzer Hitachi 917.

Glucose uptake

For monitoring glucose uptake, cells were stained with the fluorescent glucose analog 2-(*N*-(7-nitrobenz-2-oxa-1,3-diazol-4-yl)amino)-2-deoxyglucose (2-NBDG). Cells were seeded in 24-well plates and incubated with 0.1, 0.5, and 1 mM 2-NBDG for 10 min and 1 h. Then cells were washed twice with cold PBS, trypsinated, and resuspended in PBS containing 10% FCS. After centrifugation, the pellet was resolved in PBS with 10% FCS, and cells were analyzed by flow cytometry in a BD Canto II using the FITC channel.

Detection of ROS

Intracellular oxidative stress was measured by staining of the cells with the cell-permeable H_2DCFDA-AM. H_2DCFDA-AM is converted by cellular esterases to H_2DCFDA, an intermediate that oxidizes to the fluorescent 2′,7′-dichlorodihydrofluorescein (DCF) in the presence of ROS. Cells were washed with PBS and incubated for 30 min with 10 μM H_2DCFDA dissolved in PBS. After incubation, cells were washed twice with PBS and trypsinated, and the pellet was resuspended in PBS. The fluorescence signal was measured by FACS analysis using the FITC channel.

Tetramethylrhodamine (TMRM) FACS

Tetramethylrhodamine methyl ester perchlorate is a membrane-permeable cationic red-orange fluorescent dye that accumulates in active mitochondria. Therefore, cells with depolarized mitochondria have a lower signal. Cells were seeded in 24-well plates for 24 h and incubated with DMEM containing FCS or SFM for an additional 24 h. Culture medium was removed, and 25 nM TMRM dissolved in PBS was added to the cells and incubated for 45 min. Thereafter, cells were washed twice and resuspended with PBS and directly measured by FACS analysis using the phycoerythrin channel.

Proliferation assay

Cell proliferation was done with the Cell Proliferation ELISA, BrdU (colorimetric) kit from Roche Applied Science according to the supplier protocol. Cells were cultured with normal DMEM culture medium and incubated with BrdU reagent for 24 h. Experiments were performed in quadruplets.

Migration assay

For migration analysis, Corning® Transwell® polycarbonate membrane inserts (Corning, NY) were used. The transwell plates are composed of uncoated 8-μm pore polycarbonate membranes. Cells were cultured without FCS 1 day before starting the experiment, and the plate was equilibrated overnight. The next day, the lower well was filled with 600 μl of DMEM without FCS and 10 ng of fibronectin. The upper well was filled with 0.5×10^5 cells in 100 μl of 2 mM glucose in SFM. The experiment was done in triplicates for each cell line. Transwell plates were incubated overnight. The migrated cells in the lower chamber were collected 16 h following seeding. Medium residuals were removed from the upper well, and the cells attached at the bottom of the inserts were washed with PBS and stained with crystal violet. After several washing steps, polycarbonate membranes were cut out with a scalpel, embedded, and analyzed by microscopy. Ten fields of each well were counted by ImageJ and presented as mean ± S.D. ($n = 3$).

Metabolomic analysis

Cells were seeded in a density of 300,000 cells per well in 6-well plates and allowed to attach for 24 h. Then the medium was replaced by serum-free DMEM containing 25 mM glucose, and cells were incubated at 21 or 0.1% oxygen for an additional 24 h. Samples were processed as described previously (7).

Crystal violet staining

Crystal violet is a triarylmethane dye that is used to stain adherent cells as an indicator for cell density and thus for cell viability (57). For better comparison of different cell lines, cells were stained with crystal violet to ensure the same cell density at the beginning of the individual experiment. To analyze H_2O_2 sensitivity of the SCRsh and PGC-1αsh cells, cells were seeded in 24-well plates and treated with 0.8 mM H_2O_2 solution for 4 h in normal DMEM (containing 10% FCS and 25 mM glucose). Cells were stained with crystal violet when they showed the beginning signs of cell death. For cell growth analysis, cells were seeded in quadruplets in 96-well plates. DMEM (containing FCS) was freshly replaced before starting the experiment. After that, the cells were incubated for 24, 48, and 72 h and stained at each time point. After staining and fixation, the absorbance at 595 nm was measured by a multiscan photometer.

Histology and immunohistochemistry

We analyzed formalin-fixed paraffin-embedded tissue (FFPE) obtained from the mice used in the animal experiment. All blocks were stored at room temperature. For histological evaluation, 3-μm-thick slices of these FFPE blocks were performed. H&E staining was performed according to established protocols. Immunohistochemistry for Ki67 (dilution 1:100, clone SP6, ab16667, Abcam, Cambridge, UK) was performed using a standardized staining protocol on the automated immunohistochemistry staining system Leica Bond III (Leica Biosystems, Nussloch, Germany). Cell size measurement was performed using FFPE cell pellets of either SCRsh or PGC-1αsh. Images were analyzed using Olympus BX 80 light microscope and analysis software (Olympus).

In vivo glioblastoma model

For the U343MG orthotopic glioblastoma xenograft models, 5-week-old female athymic nude mice (Hsd:Athymic nude-Foxn1^{nu}) were purchased from Envigo (Indianapolis, IN) and acclimated in our animal facility for 1 week upon delivery. All animal experiments were approved by the competent local government committee (Regierungspräsidium Darmstadt, Darmstadt, Germany) and were conducted according to the applicable guidelines and regulations (National Institutes of Health Guide for the Care and Use of Laboratory Animals, GV-SOLAS). The athymic nude mice were housed on a 12-h light/dark cycle with access to food and water *ad libitum*. All animal experiments were performed unblinded. 6-Week-old mice received buprenorphine for pain relief, were anesthetized with ketamine and xylazine, immobilized in a stereotaxic fixation device (Stoelting, Wood Dale, IL), and injected through a burr hole in the skull with 5×10^5 U343MG (either SCRsh or PGC-1αsh) cells in 2 μl of PBS using a 10-μl Hamilton syringe (Hamilton, Bonaduz, Switzerland) and a Quintessential Stereotaxic Injector (Stoelting). Cells were injected at a speed of 0.5 μl per min into the right striatum with a depth of 4 mm relative to the skull surface. To avoid cell extrusion, the needle was left in place for 2 min before withdrawal at a speed of 1 mm per min. The mice were observed twice daily and sacrificed when they developed neurological symptoms or lost more than 20% of body weight.

In silico analysis

The correlation of PGC-1α with overall survival of patients and with the EGFR expression level was performed using glioblastoma samples and the dataset "Tumor Glioblastoma–TCGA–540–MAS5.0–u133a" in the R2 database using overall survival data and the 1st quartile of gene expression as a cutoff parameter. Expression analysis of PGC-1α across glioma grades II, III, and IV (glioblastomas) was analyzed using the TCGA_GBMLGG dataset and the GLIOVIS platform (58). The expression analysis of PGC-1α in nontumor tissue and glioblastomas was analyzed using the Rembrandt dataset and the GLIOVIS platform (58). Significance was tested using Tukey's range test.

Statistics

If not otherwise noted, *in vitro* experiments were done in triplicates and presented as mean ± S.D. One representative experiment out of three experiments with similar results is shown. Values were compared by two-tailed Student's *t* test (Excel, Microsoft, Seattle, WA). Values of *, $p < 0.05$ were considered significant; **, $p < 0.01$ highly significant; and values of $p > 0.05$ were considered not significant (*n.s.*). In the animal experiments, symptom-free survival was analyzed by Kaplan-Meier plot and log-rank (Mantel-Cox) test.

Author contributions—I. B., B. S., A.-L. L., M. W. R., J. P. S., and J. R. conceptualization; I. B., B. S., A.-L. L., M. W. R., J. P. S., and J. R. data curation; I. B., B. S., A.-L. L., M. W. R., J. P. S., and J. R. software; I. B., B. S., M. C. B., J. E., A.-L. L., M. W. R., J. P. S., and J. R. formal analysis; I. B., B. S., A.-L. L., M. W. R., J. P. S., and J. R. supervision; I. B., B. S., M. W. R., J. P. S., and J. R. funding acquisition; I. B., B. S., M. W. R., J. P. S., and J. R. validation; I. B., B. S., M. C. B., J. E., U. H., Y. B., P. N. H., A.-L. L., M. W. R., J. P. S., and J. R. investigation; I. B., B. S., M. C. B., J. E., A.-L. L., M. W. R., J. P. S., and J. R. visualization; I. B., B. S., M. C. B., J. E., U. H., Y. B., P. N. H., A.-L. L., M. W. R., J. P. S., and J. R. methodology; I. B., B. S., M. C. B., J. E., A.-L. L., M. W. R., J. P. S., and J. R. writing-original draft; I. B., B. S., A.-L. L., M. W. R., J. P. S., and J. R. project administration; I. B., B. S., M. C. B., J. E., A.-L. L., M. W. R., J. P. S., and J. R. writing-review and editing; M. W. R., J. P. S., and J. R. resources.

Acknowledgments—For in silico analysis the on-line database R2: Genomics Analysis and Visualization Platform, Department of Oncogenomics, Academic Medical Center (AMC), UvA, the Netherlands, was used. The Dr. Senckenberg Institute of Neurooncology is supported by the Hertie Foundation and the Dr. Senckenberg Foundation.

References

1. Elstrom, R. L., Bauer, D. E., Buzzai, M., Karnauskas, R., Harris, M. H., Plas, D. R., Zhuang, H., Cinalli, R. M., Alavi, A., Rudin, C. M., and Thompson, C. B. (2004) Akt stimulates aerobic glycolysis in cancer cells. *Cancer Res.* **64,** 3892–3899 CrossRef Medline
2. Pavlova, N. N., and Thompson, C. B. (2016) The emerging hallmarks of cancer metabolism. *Cell Metab.* **23,** 27–47 CrossRef Medline
3. Wanka, C., Brucker, D. P., Bähr, O., Ronellenfitsch, M., Weller, M., Steinbach, J. P., and Rieger, J. (2012) Synthesis of cytochrome *c* oxidase 2: a p53-dependent metabolic regulator that promotes respiratory function and protects glioma and colon cancer cells from hypoxia-induced cell death. *Oncogene* **31,** 3764–3776 CrossRef Medline
4. Wanka, C., Steinbach, J. P., and Rieger, J. (2012) Tp53-induced glycolysis and apoptosis regulator (TIGAR) protects glioma cells from starvation-induced cell death by up-regulating respiration and improving cellular redox homeostasis. *J. Biol. Chem.* **287,** 33436–33446 CrossRef Medline
5. Hartel, I., Ronellenfitsch, M., Wanka, C., Wolking, S., Steinbach, J. P., and Rieger, J. (2016) Activation of AMP-activated kinase modulates sensitivity of glioma cells against epidermal growth factor receptor inhibition. *Int. J. Oncol.* **49,** 173–180 CrossRef Medline
6. Ronellenfitsch, M. W., Brucker, D. P., Burger, M. C., Wolking, S., Tritschler, F., Rieger, J., Wick, W., Weller, M., and Steinbach, J. P. (2009) Antagonism of the mammalian target of rapamycin selectively mediates metabolic effects of epidermal growth factor receptor inhibition and protects human malignant glioma cells from hypoxia-induced cell death. *Brain* **132,** 1509–1522 CrossRef Medline
7. Thiepold, A.-L., Lorenz, N. I., Foltyn, M., Engel, A. L., Divé, I., Urban, H., Heller, S., Bruns, I., Hofmann, U., Dröse, S., Harter, P. N., Mittelbronn, M., Steinbach, J. P., and Ronellenfitsch, M. W. (2017) Mammalian target of rapamycin complex 1 activation sensitizes human glioma cells to hypoxia-induced cell death. *Brain* **140,** 2623–2638 CrossRef Medline
8. Knutti, D., and Kralli, A. (2001) PGC-1, a versatile coactivator. *Trends Endocrinol. Metab.* **12,** 360–365 CrossRef Medline

9. Wu, Z., Puigserver, P., Andersson, U., Zhang, C., Adelmant, G., Mootha, V., Troy, A., Cinti, S., Lowell, B., Scarpulla, R. C., and Spiegelman, B. M. (1999) Mechanisms controlling mitochondrial biogenesis and respiration through the thermogenic coactivator PGC-1. *Cell* **98,** 115–124 CrossRef Medline
10. LeBleu, V. S., O'Connell, J. T., Gonzalez Herrera, K. N., Wikman, H., Pantel, K., Haigis, M. C., de Carvalho, F. M., Damascena, A., Domingos Chinen, L. T., Rocha, R. M., Asara, J. M., and Kalluri, R. (2014) PGC-1α mediates mitochondrial biogenesis and oxidative phosphorylation in cancer cells to promote metastasis. *Nat. Cell Biol.* **16,** 992–1003, 1–15 CrossRef Medline
11. Yoon, J. C., Puigserver, P., Chen, G., Donovan, J., Wu, Z., Rhee, J., Adelmant, G., Stafford, J., Kahn, C. R., Granner, D. K., Newgard, C. B., and Spiegelman, B. M. (2001) Control of hepatic gluconeogenesis through the transcriptional coactivator PGC-1. *Nature* **413,** 131–138 CrossRef Medline
12. Puigserver, P., Wu, Z., Park, C. W., Graves, R., Wright, M., and Spiegelman, B. M. (1998) A cold-inducible coactivator of nuclear receptors linked to adaptive thermogenesis. *Cell* **92,** 829–839 CrossRef Medline
13. Lehman, J. J., Barger, P. M., Kovacs, A., Saffitz, J. E., Medeiros, D. M., and Kelly, D. P. (2000) Peroxisome proliferator-activated receptor γ coactivator-1 promotes cardiac mitochondrial biogenesis. *J. Clin. Invest.* **106,** 847–856 CrossRef Medline
14. Teng, C. T., Li, Y., Stockton, P., and Foley, J. (2011) Fasting induces the expression of PGC-1α and ERR isoforms in the outer stripe of the outer medulla (OSOM) of the mouse kidney. *PLoS ONE* **6,** e26961 CrossRef Medline
15. Puigserver, P., Adelmant, G., Wu, Z., Fan, M., Xu, J., O'Malley, B., and Spiegelman, B. M. (1999) Activation of PPARγ coactivator-1 through transcription factor docking. *Science* **286,** 1368–1371 CrossRef Medline
16. Puigserver, P. (2005) Tissue-specific regulation of metabolic pathways through the transcriptional coactivator PGC1-α. *Int. J. Obes. (Lond.)* **29,** Suppl. 1, S5–S9 CrossRef Medline
17. Jäger, S., Handschin, C., St-Pierre, J., and Spiegelman, B. M. (2007) AMP-activated protein kinase (AMPK) action in skeletal muscle via direct phosphorylation of PGC-1α. *Proc. Natl. Acad. Sci. U.S.A.* **104,** 12017–12022 CrossRef Medline
18. Li, X., Monks, B., Ge, Q., and Birnbaum, M. J. (2007) Akt/PKB regulates hepatic metabolism by directly inhibiting PGC-1α transcription coactivator. *Nature* **447,** 1012–1016 CrossRef Medline
19. Puigserver, P., Rhee, J., Lin, J., Wu, Z., Yoon, J. C., Zhang, C. Y., Krauss, S., Mootha, V. K., Lowell, B. B., and Spiegelman, B. M. (2001) Cytokine stimulation of energy expenditure through p38 MAP kinase activation of PPARγ coactivator-1. *Mol. Cell* **8,** 971–982 CrossRef Medline
20. Anderson, R. M., Barger, J. L., Edwards, M. G., Braun, K. H., O'Connor, C. E., Prolla, T. A., and Weindruch, R. (2008) Dynamic regulation of PGC-1α localization and turnover implicates mitochondrial adaptation in calorie restriction and the stress response. *Aging Cell* **7,** 101–111 CrossRef Medline
21. Steinbach, J. P., Klumpp, A., Wolburg, H., and Weller, M. (2004) Inhibition of epidermal growth factor receptor signaling protects human malignant glioma cells from hypoxia-induced cell death. *Cancer Res.* **64,** 1575–1578 CrossRef Medline
22. Lin, J., Tarr, P. T., Yang, R., Rhee, J., Puigserver, P., Newgard, C. B., and Spiegelman, B. M. (2003) PGC-1β in the regulation of hepatic glucose and energy metabolism. *J. Biol. Chem.* **278,** 30843–30848 CrossRef Medline
23. Schreiber, S. N., Emter, R., Hock, M. B., Knutti, D., Cardenas, J., Podvinec, M., Oakeley, E. J., and Kralli, A. (2004) The estrogen-related receptor α (ERRα) functions in PPARγ coactivator 1α (PGC-1α)-induced mitochondrial biogenesis. *Proc. Natl. Acad. Sci. U.S.A.* **101,** 6472–6477 CrossRef Medline
24. Michael, L. F., Wu, Z., Cheatham, R. B., Puigserver, P., Adelmant, G., Lehman, J. J., Kelly, D. P., and Spiegelman, B. M. (2001) Restoration of insulin-sensitive glucose transporter (GLUT4) gene expression in muscle cells by the transcriptional coactivator PGC-1. *Proc. Natl. Acad. Sci. U.S.A.* **98,** 3820–3825 CrossRef Medline
25. Vannucci, S. J., Seaman, L. B., and Vannucci, R. C. (1996) Effects of hypoxia-ischemia on GLUT1 and GLUT3 glucose transporters in immature rat brain. *J. Cereb. Blood Flow Metab.* **16,** 77–81 CrossRef Medline
26. Evans, A., Bates, V., Troy, H., Hewitt, S., Holbeck, S., Chung, Y. L., Phillips, R., Stubbs, M., Griffiths, J., and Airley, R. (2008) Glut-1 as a therapeutic target: increased chemoresistance and HIF-1-independent link with cell turnover is revealed through COMPARE analysis and metabolomic studies. *Cancer Chemother. Pharmacol.* **61,** 377–393 CrossRef Medline
27. Liu, Y., Li, Y. M., Tian, R. F., Liu, W. P., Fei, Z., Long, Q. F., Wang, X. A., and Zhang, X. (2009) The expression and significance of HIF-1α and GLUT-3 in glioma. *Brain Res.* **1304,** 149–154 CrossRef Medline
28. Arany, Z., Foo, S. Y., Ma, Y., Ruas, J. L., Bommi-Reddy, A., Girnun, G., Cooper, M., Laznik, D., Chinsomboon, J., Rangwala, S. M., Baek, K. H., Rosenzweig, A., and Spiegelman, B. M. (2008) HIF-independent regulation of VEGF and angiogenesis by the transcriptional coactivator PGC-1α. *Nature* **451,** 1008–1012 CrossRef Medline
29. Laplante, M., and Sabatini, D. M. (2009) mTOR signaling at a glance. *J. Cell Sci.* **122,** 3589–3594 CrossRef Medline
30. Keibler, M. A., Wasylenko, T. M., Kelleher, J. K., Iliopoulos, O., Vander Heiden, M. G., and Stephanopoulos, G. (2016) Metabolic requirements for cancer cell proliferation. *Cancer Metab.* **4,** 16 CrossRef Medline
31. Maher, E. A., Marin-Valencia, I., Bachoo, R. M., Mashimo, T., Raisanen, J., Hatanpaa, K. J., Jindal, A., Jeffrey, F. M., Choi, C., Madden, C., Mathews, D., Pascual, J. M., Mickey, B. E., Malloy, C. R., and DeBerardinis, R. J. (2012) Metabolism of [U-^{13}C]glucose in human brain tumors *in vivo*. *NMR Biomed.* **25,** 1234–1244 CrossRef Medline
32. Marin-Valencia, I., Yang, C., Mashimo, T., Cho, S., Baek, H., Yang, X. L., Rajagopalan, K. N., Maddie, M., Vemireddy, V., Zhao, Z., Cai, L., Good, L., Tu, B. P., Hatanpaa, K. J., Mickey, B. E., *et al.* (2012) Analysis of tumor metabolism reveals mitochondrial glucose oxidation in genetically diverse human glioblastomas in the mouse brain *in vivo*. *Cell Metab.* **15,** 827–837 CrossRef Medline
33. Lin, H., Patel, S., Affleck, V. S., Wilson, I., Turnbull, D. M., Joshi, A. R., Maxwell, R., and Stoll, E. A. (2017) Fatty acid oxidation is required for the respiration and proliferation of malignant glioma cells. *Neuro. Oncol.* **19,** 43–54 CrossRef Medline
34. Di, K., Lomeli, N., Wood, S. D., Vanderwal, C. D., and Bota, D. A. (2016) Mitochondrial Lon is over-expressed in high-grade gliomas and mediates hypoxic adaptation: potential role of Lon as a therapeutic target in glioma. *Oncotarget* **7,** 77457–77467 Medline
35. Haq, R., Shoag, J., Andreu-Perez, P., Yokoyama, S., Edelman, H., Rowe, G. C., Frederick, D. T., Hurley, A. D., Nellore, A., Kung, A. L., Wargo, J. A., Song, J. S., Fisher, D. E., Arany, Z., and Widlund, H. R. (2013) Oncogenic BRAF regulates oxidative metabolism via PGC1α and MITF. *Cancer Cell* **23,** 302–315 CrossRef Medline
36. Vazquez, F., Lim, J. H., Chim, H., Bhalla, K., Girnun, G., Pierce, K., Clish, C. B., Granter, S. R., Widlund, H. R., Spiegelman, B. M., and Puigserver, P. (2013) PGC1α expression defines a subset of human melanoma tumors with increased mitochondrial capacity and resistance to oxidative stress. *Cancer Cell* **23,** 287–301 CrossRef Medline
37. Zhu, L., Wang, Q., Zhang, L., Fang, Z., Zhao, F., Lv, Z., Gu, Z., Zhang, J., Wang, J., Zen, K., Xiang, Y., Wang, D., and Zhang, C. Y. (2010) Hypoxia induces PGC-1α expression and mitochondrial biogenesis in the myocardium of TOF patients. *Cell Res.* **20,** 676–687 CrossRef Medline
38. Santos, J. M., Tewari, S., and Benite-Ribeiro, S. A. (2014) The effect of exercise on epigenetic modifications of PGC1: the impact on type 2 diabetes. *Med. Hypotheses* **82,** 748–753 CrossRef Medline
39. Shah, K., Desilva, S., and Abbruscato, T. (2012) The role of glucose transporters in brain disease: diabetes and Alzheimer's disease. *Int. J. Mol. Sci.* **13,** 12629–12655 CrossRef Medline
40. Yeh, W. L., Lin, C. J., and Fu, W. M. (2008) Enhancement of glucose transporter expression of brain endothelial cells by vascular endothelial growth factor derived from glioma exposed to hypoxia. *Mol. Pharmacol.* **73,** 170–177 Medline
41. St-Pierre, J., Drori, S., Uldry, M., Silvaggi, J. M., Rhee, J., Jäger, S., Handschin, C., Zheng, K., Lin, J., Yang, W., Simon, D. K., Bachoo, R., and Spiegelman, B. M. (2006) Suppression of reactive oxygen species and neu-

rodegeneration by the PGC-1 transcriptional coactivators. *Cell* **127,** 397–408 CrossRef Medline

42. Marmolino, D., Manto, M., Acquaviva, F., Vergara, P., Ravella, A., Monticelli, A., and Pandolfo, M. (2010) PGC-1α down-regulation affects the antioxidant response in Friedreich's ataxia. *PLoS ONE* **5,** e10025 CrossRef Medline
43. Fu, X. F., Yao, K., Du, X., Li, Y., Yang, X. Y., Yu, M., Li, M. Z., and Cui, Q. H. (2016) PGC-1α regulates the cell cycle through ATP and ROS in CH1 cells. *J. Zhejiang Univ. Sci. B* **17,** 136–146 CrossRef Medline
44. Liou, G. Y., and Storz, P. (2010) Reactive oxygen species in cancer. *Free Radic. Res.* **44,** 479–496 CrossRef Medline
45. Ristow, M., and Schmeisser, K. (2014) Mitohormesis: promoting health and lifespan by increased levels of reactive oxygen species (ROS). *Dose Response* **12,** 288–341 Medline
46. Scherz-Shouval, R., Shvets, E., Fass, E., Shorer, H., Gil, L., and Elazar, Z. (2007) Reactive oxygen species are essential for autophagy and specifically regulate the activity of Atg4. *EMBO J.* **26,** 1749–1760 CrossRef Medline
47. Lee, J., Giordano, S., and Zhang, J. (2012) Autophagy, mitochondria and oxidative stress: cross-talk and redox signalling. *Biochem. J.* **441,** 523–540 CrossRef Medline
48. Wenz, T. (2009) PGC-1α activation as a therapeutic approach in mitochondrial disease. *IUBMB Life* **61,** 1051–1062 CrossRef Medline
49. De Luca, A., Fiorillo, M., Peiris-Pagès, M., Ozsvari, B., Smith, D. L., Sanchez-Alvarez, R., Martinez-Outschoorn, U. E., Cappello, A. R., Pezzi, V., Lisanti, M. P., and Sotgia, F. (2015) Mitochondrial biogenesis is required for the anchorage-independent survival and propagation of stem-like cancer cells. *Oncotarget* **6,** 14777–14795 Medline
50. Hanahan, D., and Weinberg, R. A. (2011) Hallmarks of cancer: the next generation. *Cell* **144,** 646–674 CrossRef Medline
51. Dodd, K. M., Yang, J., Shen, M. H., Sampson, J. R., and Tee, A. R. (2015) mTORC1 drives HIF-1α and VEGF-A signalling via multiple mechanisms involving 4E-BP1, S6K1 and STAT3. *Oncogene* **34,** 2239–2250 CrossRef Medline
52. Chen, C., Pore, N., Behrooz, A., Ismail-Beigi, F., and Maity, A. (2001) Regulation of glut1 mRNA by hypoxia-inducible factor-1. Interaction between H-ras and hypoxia. *J. Biol. Chem.* **276,** 9519–9525 CrossRef Medline
53. Hayashi, M., Sakata, M., Takeda, T., Yamamoto, T., Okamoto, Y., Sawada, K., Kimura, A., Minekawa, R., Tahara, M., Tasaka, K., and Murata, Y. (2004) Induction of glucose transporter 1 expression through hypoxia-inducible factor 1α under hypoxic conditions in trophoblast-derived cells. *J. Endocrinol.* **183,** 145–154 CrossRef Medline
54. Keunen, O., Johansson, M., Oudin, A., Sanzey, M., Rahim, S. A., Fack, F., Thorsen, F., Taxt, T., Bartos, M., Jirik, R., Miletic, H., Wang, J., Stieber, D., Stuhr, L., Moen, I., *et al.* (2011) Anti-VEGF treatment reduces blood supply and increases tumor cell invasion in glioblastoma. *Proc. Natl. Acad. Sci. U.S.A.* **108,** 3749–3754 CrossRef Medline
55. Mao, X. G., Wang, C., Liu, D. Y., Zhang, X., Wang, L., Yan, M., Zhang, W., Zhu, J., Li, Z. C., Mi, C., Tian, J. Y., Hou, G. D., Miao, S. Y., Song, Z. X., Li, J. C., and Xue, X. Y. (2016) Hypoxia upregulates HIG2 expression and contributes to bevacizumab resistance in glioblastoma. *Oncotarget* **7,** 47808–47820 Medline
56. Steinbach, J. P., Wolburg, H., Klumpp, A., Probst, H., and Weller, M. (2003) Hypoxia-induced cell death in human malignant glioma cells: energy deprivation promotes decoupling of mitochondrial cytochrome c release from caspase processing and necrotic cell death. *Cell Death Differ.* **10,** 823–832 CrossRef Medline
57. Grady, J. E., Lummis, W. L., and Smith, C. G. (1960) An improved tissue culture assay. III. Alternate methods for measuring cell growth. *Cancer Res.* **20,** 1114–1117 Medline
58. Bowman, R. L., Wang, Q., Carro, A., Verhaak, R. G., and Squatrito, M. (2017) GlioVis data portal for visualization and analysis of brain tumor expression datasets. *Neuro. Oncol.* **19,** 139–141 CrossRef Medline